

THE COMPACT GROUP OF GALAXIES HCG 31 IS IN AN EARLY PHASE OF MERGING

P. AMRAM¹, C. MENDES DE OLIVEIRA^{2,3}, H. PLANA⁴, C. BALKOWSKI⁵, O. HERNANDEZ^{1,6}, C. CARIGNAN⁶, E.S. CYPRIANO^{7,8}, L. SODRÉ JR.², J.L. GACH¹ AND J. BOULESTEIX¹

Draft version November 18, 2018

ABSTRACT

We have obtained high spectral resolution ($R = 45900$) Fabry-Perot velocity maps of the Hickson Compact Group HCG 31 in order to revisit the important problem of the merger nature of the central object A+C and to derive the internal kinematics of the candidate tidal dwarf galaxies in this group. Our main findings are: (1) double kinematic components are present throughout the main body of A+C, which strongly suggests that this complex is an ongoing merger (2) regions A2 and E, to the east and south of complex A+C, present rotation patterns with velocity amplitudes of $\sim 25 \text{ km s}^{-1}$ and they counterrotate with respect to A+C, (3) region F, which was previously thought to be the best example of a tidal dwarf galaxy in HCG 31, presents no rotation and negligible internal velocity dispersion, as is also the case for region A1. HCG 31 presents an undergoing merger in its center (A+C) and it is likely that it has suffered additional perturbations due to interactions with the nearby galaxies B, G and Q.

Subject headings: galaxies: individual (HCG 31) — galaxies: kinematics and dynamics — galaxies: evolution — galaxies: interactions — galaxies: formation — instrumentation: interferometers

1. INTRODUCTION

The spectacular Hickson Compact Group 31 (Hickson 1982) shows a wide range of indicators of galaxy interaction and merging: tidal tails, irregular morphology, complex kinematics, vigorous star bursting (e.g. Rubin et al. 1990) and possible formation of tidal dwarf galaxies (e.g. Hunberger et al. 1996). All the objects belonging to the group are embedded in a common large HI envelope (Williams et al. 1991). The group is formed by members A+C, B, E, F, G, Q (Rubin et al. 1990).

Two scenarios have been put forward to explain the nature of the central system A+C: it is either two systems that are about to merge (e.g. Rubin et al. 1990) or a single interacting galaxy (Richer et al. 2003). In this Letter we use our new Fabry-Perot maps and deep imaging from Gemini-N to revisit the important problem of the merger nature of the central object of the group, A+C, and, in addition, we investigate the internal kinematics of the tidal dwarf galaxies, in an attempt to identify if they are self gravitating objects or not. We adopt a distance of 54.8 Mpc, from the redshift $z=0.0137$ (Hickson et al. 1992) and using $H_0=75 \text{ km s}^{-1} \text{ Mpc}^{-1}$, hence $1'' \sim 0.27 \text{ kpc}$.

2. OBSERVATIONS

Observations were carried out with the Fabry-Perot instrument CIGALE (Gach et al. 2002) attached to the ESO 3.6m telescope in August 2000. Interferograms were obtained with a high order ($p=1938$) Fabry-Perot scanning interferometer, giving a free spectral range of

155 km s^{-1} with a *Finesse* $F=24$ leading to a spectral resolution of $R = 45\,900$. The pixel size is 0.405 arcsec; the total exposure time was 72 min (6 cycles of 12 min each, 48 scanning steps per cycle) and the FWHM of the interference filter centered around 6651 \AA was 20 \AA . The velocity sampling was 3 km s^{-1} and the relative velocity accuracy is $\sim 1 \text{ km s}^{-1}$ over the whole field where the S/N is greater than 3. Reduction of the data cubes were performed using the CIGALE/ADHOCw software (Boulesteix, 2002). The data reduction procedure has been described e.g. in Blais-Ouellette et al. (1999) and Garrido et al. (2002). For the adopted distance of the group, one pixel corresponds to $\sim 0.11 \text{ kpc}$.

In August 2003, we obtained two images with GMOS at Gemini-N in g' and r' with exposure times of 1200 and 900 seconds respectively. These images have a pixel size of $0.14''$ and typical seeing of $0.75''$.

3. RESULTS

A color map of the group is presented in Fig. 1a. It shows a wealth of star forming regions and the large extent of the optical diffuse light which envelopes the group. For the first time, regions A1 and A2, to the east of complex A+C, are seen in great detail and depth.

Fig. 1b–d show the $H\alpha$ monochromatic map of the group, the velocity map and several zoom panels showing the typical velocity profiles in selected regions of the group. The velocity field was corrected from free spectral range ambiguity using previous kinematic observations. At a first look, galaxies A and C appear to be a single kinematic entity, as their velocity fields show no discontinuity. Under this assumption, we can infer a rough mass for the A+C complex, within a radius of $\sim 18 \text{ arcsec}$ ($\sim 4.9 \text{ kpc}$) of $M \sim 4.5 \times 10^9 M_\odot$. The following parameters and assumptions were used for this mass determination: a maximum rotational velocity of $70 \pm 10 \text{ km s}^{-1}$ (only from the NW side of the system given that the SE side is too disturbed), a kinematic in-

¹ LAM/OAMP, Marseille, France. (Philippe.Amram@oamp.fr)

² IAG, São Paulo, Brazil. (oliveira@astro.iag.usp.br)

³ Ludwig-Maximilians-Universität, München, Germany

⁴ Universidade Estadual de Santa Cruz, Ilhéus, Brazil

⁵ GEPI, CNRS et Paris 7, Meudon, France

⁶ Université de Montréal and LAE, Montréal, Québec, Canada.

⁷ Laboratório Nacional de Astrofísica, Itajubá, Brazil

⁸ Southern Astrophys. Research Telescope, La Serena, Chile

clination and position angle of 51 ± 5 and 130 ± 3 degrees respectively and the assumption that the measured motions are due to disk rotation. Nevertheless, multiple profiles (see Fig. 1d), evident almost everywhere in the main body of A+C, strongly suggests that A+C is not a single entity and therefore this rough determination provides only an order of magnitude for the mass.

Fig. 2 shows the velocity gradients of the objects A1, A2, E and F, situated around the pair A+C (see Fig 1a) and which have been thought to be candidate tidal dwarf galaxies (Hunsberger et al. 1996, Iglesias-Páramo & Vílchez 2001 and Richer et al. 2003). The curves are not corrected for inclination and the central position and velocity were chosen such that the curves were as symmetric as possible, with both sides matching, when possible. The object with the highest velocity gradient is E, with ordered velocities which range from 3950 km s^{-1} to 4000 km s^{-1} . Object A2 also shows ordered motion, with velocities going from 4125 to 4175 km s^{-1} . Surprisingly, object F, thought to be the best tidal dwarf galaxy candidate in the group, shows a completely flat rotation curve, as does also the smaller object to the northeast of A+C, fragment A1. In addition, A1 and F have low gaseous velocity dispersions. These results will be discussed in the next section.

We obtained the map of the gaseous velocity dispersion at each pixel of the image (Amram et al. 2004, in preparation) assuming the profiles are well represented by a single gaussian. The value for the velocity dispersion ranges from 10 to 30 km s^{-1} throughout the group. In particular, objects A1, A2, E and F show typical velocity dispersions of 15 km s^{-1} , which in some isolated regions can reach up to 25 km s^{-1} . The highest values for the velocity dispersion lie in the overlapping region between A and C, mainly due to double components. It is noticeable that these highest values do not match the most intense star forming regions everywhere in the galaxies but particularly where disk A and C overlap, implying that the line broadening and the multiple components are not directly linked to star formation triggered by interaction with another galaxy but specifically by the merging of A+C. Hickson & Menon (1985) reached a similar conclusion, analyzing a radio continuum map of the group. They found that the 20 cm peak of emission comes from the overlapping regions of A and C, indicating additional evidence of recent excessive starburst activity in this region.

4. DISCUSSION

4.1. *The ongoing merger A+C*

Richer et al. (2003) also presented Fabry-Perot velocity maps of HCG 31. There is fairly good general agreement between their velocity field and ours. The spectral resolution of our maps is nevertheless six times higher (7900 vs 45900) and the detection limit several magnitudes fainter. Several authors supported that A and C are separate entities in an ongoing merging phase (e.g. Vorontsov-Velyaminov and Arhipova, 1963; Rubin et al., 1990) while Richer et al. (2003) supported the scenario that A+C is a single interacting spiral galaxy. The new piece of evidence in support of the merging scenario reported in this paper is the presence of double velocity components throughout the system A+C. In fact, our

higher resolution velocity field shows kinematic structures which are not naturally explained by a single disk but by the merging of two disks.

Although Sc galaxies are, in general, transparent objects (Bosma 1995), moderate amounts of molecular gas (as traced by the CO) and cold dust may make some regions opaque. The CO emission is weak in HCG 31 but the brightest CO peak occurs in the overlapping region between galaxies A and C (Yun et al. 1997) where the broader H α profiles are observed. If the CO belongs to the foreground galaxy, multiple components are observed in regions optically thick and then could not be observed if disk A and C are two separate galaxies seen in projection, i.e. chance alignment. Multiple gaseous components are observed in the same disk plane when they are not in equilibrium (e.g. Östlin et al. 2001). This occurs when two different entities merge, or when the feedback gas due to star formation interacts with the ISM. We observe in HCG 31 the signature of both mechanisms, the second one being probably a consequence of the first one.

The general pattern of the velocity field of HCG31 A+C is somewhat similar to that of NGC 4038/9 (the Antennae, Amram et al., 1992) in which a continuity in the isovelocities between both galaxies is also observed in the overlapping region. The merging stage of the Antennae is slightly less advanced than that for A+C. In the Antennae, the two galaxies are clearly separate entities and their bodies, which are not yet overlapping, each display an increasing velocity gradient, which is roughly parallel and run from the NE to the SW (Amram et al. 1992). It is likely that when the disks of NGC 4038 and of NGC 4039 overlap, the velocity field will also present total continuity, as observed in A+C.

Galaxy C (Mrk 1089) has been classified as a double nucleus Markarian galaxy, the two nuclei being separated by 3.4 arcsec (Mazzarella & Boroson, 1993) and it is difficult to explain the existence of the two nuclei without invoking a merging scenario, as shown by numerical simulations (e.g. Barnes & Hernquist 1992). To reproduce the double line profile in NGC 4848, Vollmer et al (2001) have used numerical simulations. They interpret them as the consequence of infalling gas which collides with the ISM within the galaxy. This gives rise to an enhanced star formation observed in the H α and in the 20 cm continuum map.

HCG 31 is most probably a group in an early phase of merger, growing through slow and continuous acquisition of galaxies from the associated environment. Moreover, several evidences for interaction with the other galaxy components of the group, namely B, Q and G (e.g. the group is completely embedded in a large HI envelope showing a local maximum on G to the SW and another one around Q to the NE) indicate that the complex A+C is most probably accreting the surrounding galaxies.

4.2. *Tidal Fragments*

Several papers in the past (Hunsberger et al. 1996, Johnson and Conti 2000, Richer et al. 2003 and Iglesias-Páramo & Vílchez 2001) have mentioned the possibility that tidal dwarf galaxies in HCG 31 were formed. The best candidates are objects E and F, for which metallicities were measured and they were determined to be

similar to that of the complex A+C, suggesting a tidal origin for these objects (Richer et al., 2003).

As shown in Fig. 2, we detect ordered motions only for objects A2 and E and not for A1 and F. It might be suspected that the internal velocity motions measured in A2 and E could be due to streaming motions in incipient tidal tails in formation (see Fig. 1a). This is, however, not the case because these objects are counterrotating with respect to the main body of A+C. The discontinuity of the isovelocities can be clearly seen from Fig. 1c: the velocities go from high (northeast) to low (southwest) in A+C, towards object E. Then, along the body of E they go in the opposite sense. Similarly, for object A2, it presents counterrotation with respect to its immediate neighbor to the west: galaxy A. These objects may fall back onto their progenitor. In fact, from their velocity differences with respect to the A+C complex ($+115 \text{ km s}^{-1}$ and -60 km s^{-1} respectively) and from their relative projected distances (6.7 kpc and 5.4 kpc respectively) and assuming a total mass for the A+C complex of $M \sim 4.5 \times 10^9 M_{\odot}$, we could determine that these two objects will indeed, most probably, fall back onto A+C. The same is true for object F, which although more distant from A+C, has a very small radial velocity difference of $\sim 60 \text{ km s}^{-1}$. We note, however, that given the fact that we measure radial velocities (and not the velocity component in the plane of the sky), the observed internal velocities of the tidal fragments are lower limits.

Region F, which was previously thought to be the best example of a tidal dwarf galaxy in HCG 31, is indeed part of the main merger, following the same kinematic pattern of the parent galaxy and presenting no rotation nor significant internal velocity dispersion. Region F was found to have low or inexistent old stellar population by Johnson and Conti (2000). If there is no old stellar population the velocity dispersion of the gas is mainly indicating the dynamics of the cloud. The range of values derived for the internal velocity dispersion of F, $15\text{-}25 \text{ km s}^{-1}$, is too close to the natural turbulence of the gas and/or the expanding velocity due to starburst winds. The lack of rotation and the continuity of the kinematics between the main body of the merger and object F suggest it is simply a tidal debris, although, considering its projected

distance from A+C (16 kpc) and the large amount of fuel available in the whole area of the merger ($2.1 \times 10^{10} M_{\odot}$ of HI gas), it could perhaps develop into a tidal dwarf galaxy in the future, by accretion of infalling material.

There is also the possibility that regions A1 and F present no velocity gradient due to their rotation pattern be along the line of sight. Although this could be a possibility for the smaller and rounder region A1, it is less likely the case for region F, given its elongated morphology.

5. CONCLUSIONS

Our two main results are:

1) We measure multiple kinematic components throughout the body of A+C which we interpret as a strong indication that this complex is an ongoing merger. The double photometric nucleus has been identified in several previous images of HCG 31 including the spectacular HST image published by Johnson and Conti (2000) and in Fig. 1a. The double kinematic component is shown here for the first time in Fig. 1d.

2) F and A1 present flat rotation velocity profiles and insignificant velocity dispersions. In contrast, A2 and E are structures counterrotating with respect to the parent A+C complex.

We conclude that HCG 31 is a merging group which is probably going to soon end up as a field elliptical galaxy. It would be very valuable to compare our new, high spectral resolution maps to simulations of groups to investigate which interaction and merger parameters fit these data.

The authors thank Olivier Boissin for help during the observations, Jorge Iglesias-Páramo for kindly providing the calibrated H α image and to acknowledge financial support from the French-Brazilian PICS program. CMdO, LS and ESC would like to thank the Brazilian PRONEX program, FAPESP, CNPq. CMdO deeply acknowledges the funding and hospitality of the MPE Institut in Garching, where this work was finalized. CC and OH acknowledge support from FQRNT, Québec and NSERC, Canada.

REFERENCES

- Amram P., Marcelin M., Boulesteix J. et al 1992, A&A, 266, 106
 Amram P., Mendes de Oliveira C., Boulesteix J. et al. 1998, A&A, 330, 881
 Blais-Ouellette S.; Carignan C., Amram P. et al, 1999, AJ, 118, 2123
 Boulesteix J., 2002, ADHOCw Red.Package, www.oamp.fr/adhoc/
 Bosma A., 1995 in NATO Advanced Science Inst. Ser. C, 469, 317
 Gach J.-L., Hernandez O., Boulesteix J. et al. 2002, PASP, 114, 1043
 Garrido O., Marcelin M., Amram P. et al, 2002, A&A, 387, 821
 Hickson P. 1982, ApJ, 255, 382
 Hickson P., Mendes de Oliveira C., Huchra J.P. et al. 1992, ApJ 399,353
 Hickson P. & Menon T.K. 1985, ApJ 296, 60
 Hunsberger S.D., Charlton J.C. & Zaritsky D. 1996, ApJ 462, 50
 Iglesias-Páramo J. & Vílchez J.M. 2001, ApJ 550, 204
 Johnson K.E. & Conti P.S. 2000, AJ 119, 2146
 Östlin G., Amram P., Bergvall N. et al. 2001, A&A 374, 800
 Richer M.G., Georgiev L., Rosado M. et al., 2003, A&A, 397, 99
 Rubin V.C., Hunter D.A., Ford W.K.Jr. 1990, ApJ, 365, 86
 Vollmer B., Braine J., Balkowski C. et al., 2001, A&A,374,824
 Vorontsov-Velyaminov B.A. & Arhipova, Trudy G. Astron. Inst. Sht., 33, 1, 1963
 Williams B.A., McMahon P.M., van Gorkom J.H., 1991, AJ, 101, 1957
 Yun M.S., Verdes-Montenegro L., del Olmo A. et al., 1997, ApJ, 475L,21.

FIG. 1.— *HCG 31*. **Upper Left, Fig. 1a:** Composite g' and r' color image of the central region of the group. **Upper Right, Fig. 1b:** net- $H\alpha$ map. The flux is given in a logarithmic scale, in units of $10^{-16} \text{ erg s}^{-1} \text{ arcsec}^{-2} \text{ cm}^{-2}$, the calibration has been done with the $H\alpha$ image from Iglesias-Páramo & Vílchez (2001). The four small open squares labeled 11, 12, 21, 22 are the windows within which the profiles shown in Fig. 1d have been extracted. Their size are 8×8 pixels. ($\sim 3.2'' \times 3.2''$ or $\sim 0.9 \text{ kpc} \times 0.9 \text{ kpc}$). **Bottom Left, Fig. 1c:** $H\alpha$ velocity field; the scale is labeled in km s^{-1} and the black isocontours are separated by 25 km s^{-1} . **Bottom Right, Fig. 1d:** Examples of velocity profiles corresponding to the windows displayed on the $H\alpha$ image (Fig. 1b). Each small box represents 2×2 pixels ($\sim 0.8'' \times 0.8''$ or $\sim 0.22 \text{ kpc} \times 0.22 \text{ kpc}$) on the sky. The origin of the X-axis corresponds to 6648 \AA (3917 km s^{-1}) and the amplitude of the x -axis represents the $\sim 3.5 \text{ \AA}$ free spectral range of the interferometer ($\sim 155 \text{ km s}^{-1}$). The profiles are plotted without correction for possible free spectral range jump: velocity differences between various components may be the value plotted in the figure plus $n \times 155 \text{ km s}^{-1}$ (n being an integer, positive or negative). The intensities of the profiles have been normalized to the brightest one. The color background pixels correspond to the intensities displayed on the $H\alpha$ image.

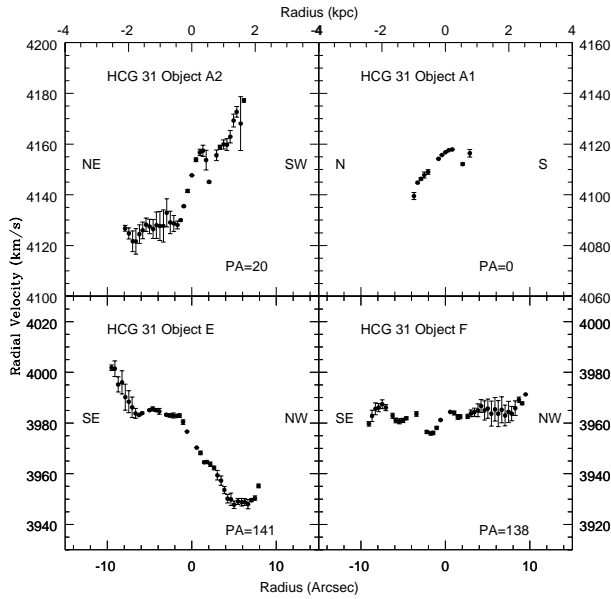


FIG. 2.— Velocity gradients for the tidal dwarf galaxy candidates

This figure "amram_fig1a.gif" is available in "gif" format from:

<http://arxiv.org/ps/astro-ph/0407525v2>

This figure "amram_fig1b.gif" is available in "gif" format from:

<http://arxiv.org/ps/astro-ph/0407525v2>

This figure "amram_fig1c.gif" is available in "gif" format from:

<http://arxiv.org/ps/astro-ph/0407525v2>

This figure "amram_fig1d.gif" is available in "gif" format from:

<http://arxiv.org/ps/astro-ph/0407525v2>